# Open Research Online

The Open University

The Open University's repository of research publications
and other research outputs

# Validation of NIEL for 1MeV electrons in silicon using the CCD47-20

## Conference or Workshop Item

# oro.open.ac.uk

# Validation of NIEL for >1 MeV electrons in silicon using the CCD47-20

B. Dryer*[a], P. H. Smith[a], T. Nuns[b], N. J. Murray[a,c], K. D. Stefanov[a],
J. P. D. Gow[a], R. Burgon[a], D. J. Hall[a], A. D. Holland[a]

[a]Centre for Electronic Imaging, The Open University, Walton Hall, Milton Keynes, MK7 6AA, UK
[b]ONERA, 2 Avenue Edouard Belin, FR-31055, Toulouse, Cedex 4, France

## ABSTRACT

For future space missions that are visiting hostile electron radiation environments, such as ESA's JUICE mission, it is important to understand the effects of electron irradiation on silicon devices. This paper outlines a study to validate and improve upon the Non-Ionising Energy Loss (NIEL) model for high energy electrons in silicon using Charge Coupled Devices (CCD), CMOS Imaging Sensors (CIS) and PIPS photodiodes. Initial results of radiation effects in an e2v technologies CCD47-20 after irradiation to 10 krad of 1 MeV electrons are presented with future results and analysis to be presented in future publications.

**Keywords:** CCD, NIEL, Non-ionising energy loss, radiation effects, electron, silicon, proton, gamma

## 1. INTRODUCTION

### Non-Ionising Energy Loss (NIEL)

Damage to semiconductor devices is caused by ionising and non-ionising energy transfer mechanisms induced by incident particles. Ionising damage causes electron-hole pairs to be liberated from the material lattice, either by coulombic interactions with a particle or by photoelectric liberation by a photon. This becomes a problem when the electrons (and holes) are liberated in a region that they cannot be efficiently drained from e.g. regions of insulator. The damage effects caused by ionising damage scale with the Total Ionising Dose (TID). In contrast displacement damage is caused by the liberation of an atom from the crystal lattice by a particle with sufficiently high kinetic energy. In the same way, effects caused by displacement damage scale with the Non-Ionising Energy Loss (NIEL), a scaling factor that relates a particle's rate of energy loss to displacement effects as it passes through a material. Figure 1 shows measured NIEL factors for protons, neutrons, electrons and pions across a range of energies. Using these factors, it is possible to simplify a complex radiation environment such as those found naturally in space, and to simulate them and study damage to devices via irradiation by a single particle species, scaled using TID and NIEL.

### Understanding Electron NIEL in Silicon Devices

While the NEIL model is useful in the planning of irradiation campaigns and creating analogues of the complex space radiation environment on Earth, there are occasions where the model deviates significantly from observed damage effects, for example in GaAs devices irradiated with protons above 40 MeV [8]. The NIEL model has been studied in detail and validated for common particle species in Earth orbits (e.g. 10 MeV protons), but has been less thoroughly studied for particles that may be common in more exotic environments, such as the high energy (>10 MeV) electrons found in belts around Jupiter.

*ben.dryer@open.ac.uk; phone (+44)1908 898199; open.ac.uk/cei
[c]now at Dynamic Imaging Analytics Limited, Bletchley Park Science and Innovation Centre, Milton Keynes, MK3 6EB, UK

Recent evidence has suggested that electron NIEL may deviate significantly from existing models [3-5]. However, new models that correctly predict the damage at low electron energies can greatly overestimate the damage at higher energies. Figure 2 shows the 'classical' NIEL model compared to a new model which scales damage quadratically with electron energy [6]. Understanding how high energy electron displacement damage deviates from the classical NIEL model is essential for correctly estimating the damage to the focal plane of upcoming missions, e.g. the ESA Horizons 2020 mission to the Jovian system, JUICE [7].
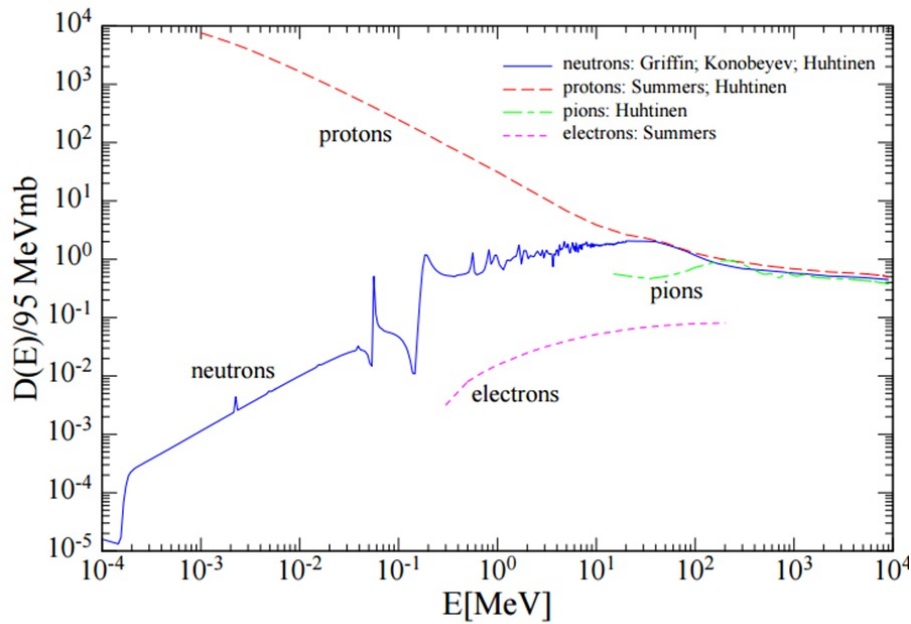


Figure 1. Displacement damage in silicon for neutrons, protons, pions and electrons. [1]
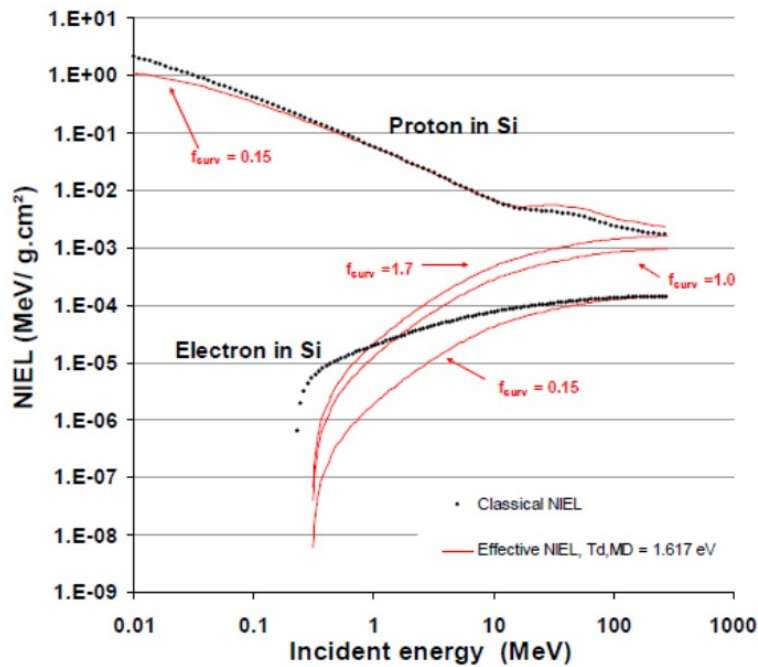


Figure 2. NIEL model[10] from Summers compared to refined model for electron damage. [2]

## 2. METHODS

**The CCD47-20**

The device selected for the CCD part of the study is the CCD47-20[9], a three-phase frame transfer CCD comprised of 1024 × 1024 13 μm square image area pixels, and is capable of running in AIMO mode to lower dark current. The CCD 47-20 is commercially available in front and back illuminated variants. The device was chosen for this study due to the low dark current (suppressed by AIMO) and readout noise, and relative availability of the devices for use in the study. The CCD 47-20 also has significant space heritage in star trackers, meaning that there is an abundance of radiation data available on these devices for comparison later in the study. Figures 3 and 4 show a photograph and a schematic of the device respectively.
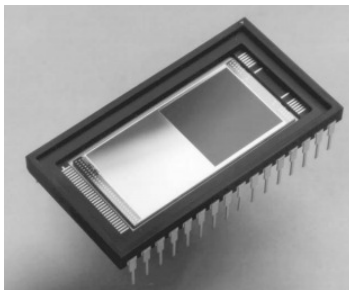


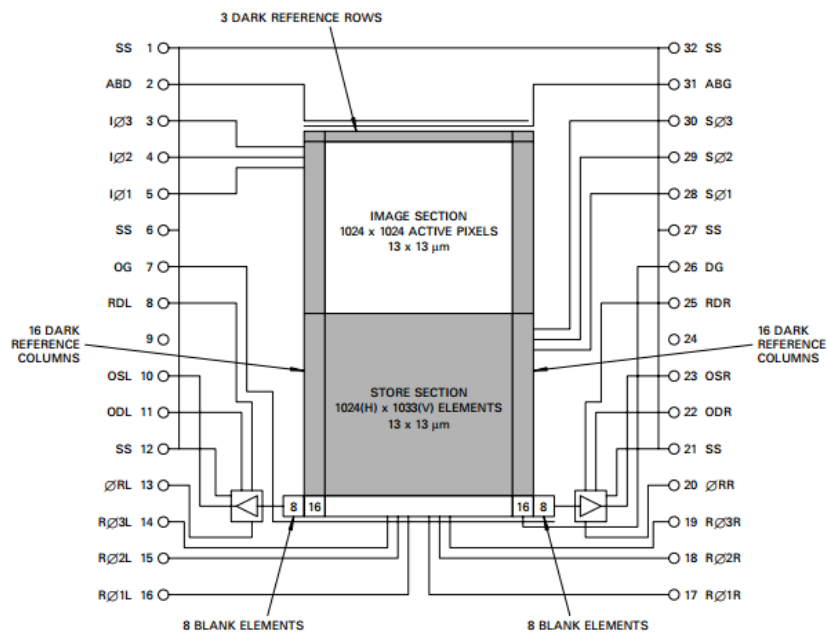Figure 3. A photograph of the e2v technologies CCD47-20.[9]



Figure 4. A schematic of the CCD47-20, showing bias and clock connections, as well as the pixel layout of the device. [9]

**High Energy Electron NIEL Study Plan**

The study as a whole is concerned with validating the NIEL of high energy electrons in a variety of device architectures, specifically the CCD through e2v technologies CCD47-20, the CIS through e2v technologies EV76C560 "Sapphire" CMOS Imaging Sensor (CIS), and the PIPS Photodiode through the Canberra FD50-14-300RM PIPS Photodiode. The different architecture of these devices will help to identify any device specific effects that may be present and to correlate the effects of electron irradiation between these different technologies. Table 1 shows the planned irradiation species and energies for the full study. This work is accompanied by a modelling activity, which aims to validate a NIEL model

dependant on the displacement damage threshold and the recombination rate of damage in order to fit a NIEL model to the experimental data found during the study.

| Particle | Proton | | | Electron | | | | Gamma | | Control |
|---|---|---|---|---|---|---|---|---|---|---|
| **Facility** | Harwell, GB | PIF, PSI, CHE | PIF, PSI, CHE | ONERA, FRA | RADEF, FIN | RADEF, FIN | RADEF, FIN | ONERA, FRA | ONERA, FRA | - |
| **Energy (MeV)** | 6.5 | 72 | 200 | 1 | 6 | 12 | 20 | 1.17/1.33 | 1.17/1.33 | 0 |
| **Dose (krad)** | 3 | 3 | 3 | 10 | 10 | 10 | 10 | 3 | 10 | 0 |

Table 1. Particle species, dose, and planned facilities for performed and *future (italic)* irradiations for the high energy electron NIEL study.

This paper describes the details of the study, current progress, and preliminary results obtained so far on the CCD47-20 by the Open University, after an electron irradiation at 1 MeV, and proton irradiations at 72 MeV and 200 MeV. Further results will be available in the coming months, as the study progresses.

**CCD Testing Methods**

A number of different parameters are measured on the CCD 47-20 for the study. In order to completely validate the NIEL relationship, it is important to compare these different parameters, as different particle species may affect each device in subtly different ways. All devices are annealed at room temperature for 4 weeks after irradiation, ensuring that any rapid mobility of damage in the devices has settled and that the damage effects measured will be more stable in the device at that temperature. Similar device parameters are being measured, where applicable, in the CISs and PIPS photodiodes.

| Device parameter | Test Method |
|---|---|
| Dark Current | Dark current frames are taken for two integration times at five temperatures between -30°C and +15°C. |
| Dark Signal Non-Uniformity (DSNU) | Same as dark current, DSNU is reported as a percentage of mean deviation from the median signal level. |
| Charge Transfer Efficiency | A virtual knife edge is created by back clocking the device and dumping the signal in part of the image region, this gives a clean edge to the image area from which to measure CTE using the Extended Pixel Edge Response (EPER method). The leading edge of the image area is used to also measure the First Pixel Response (FPR). |
| Activation Energy of Dark Current | Derived from the gradient of an Arrhenius plot of the dark current with temperature. |
| Random Telegraph Signals | Readout of a small area of the image over 30 minutes at +15°C, to monitor for pixels with fluctuating dark current, detected with an edge detection filter. |

Table 2. Summary of measured parameters and test methods for CCD 47-20 testing at the Open University.

# 3. RESULTS AND DISCUSSION

This paper concerns the preliminary results on a single irradiated CCD. Thus far only the performance of the device irradiated to 10 krad with 1 MeV electrons has been analysed due to the publish date of this paper and the ongoing nature of the study (other devices undergoing room temperature anneal). Future publications will provide much more detail on the analysis of all devices that were irradiated for the project.

As the substrate voltage was optimised pre-irradiation, there may be a need to shift the substrate voltage slightly higher to achieve full pinning of the channel away from the surface dark current, accounting for any radiation induced flat-band voltage shift. This is important to monitor especially in the case of gamma and electron irradiated devices, as the TID will be significantly higher than for a proton irradiation of the same combined TID and displacement dose.

As an example, Figure 6 shows that the substrate voltage needed to pin the device increases from 8.8 V to approximately 10 V after 10 krad of 1 MeV electrons, an increase of 120 mV·krad$^{-1}$. This also demonstrates very effectively the increased density of surface interface states, as the dark current increases two-fold under pinned conditions, but over five-fold in the unpinned surface.

Figure 7 shows the serial EPER degradation under electron irradiation at -20°C. Node 2 (*c.f.* Figure 5) was covered partially by a mask, and hence why we see a lower CTI increase here. The results suggest a five-fold increase in EPER CTI after electron irradiation to 10 krad. The higher CTI in Node 2 at low signal levels is likely due to increased errors at low light levels. The effect is currently undergoing investigation.

Figure 8 shows the Arrhenius plot for the frame and store region of the CCD for each node post 10 MeV electron irradiation. The corresponding activation energies are $0.661 \pm 0.03$ eV for the frame and $0.6294 \pm 0.06$ eV for the store regions, close to mid bandgap.
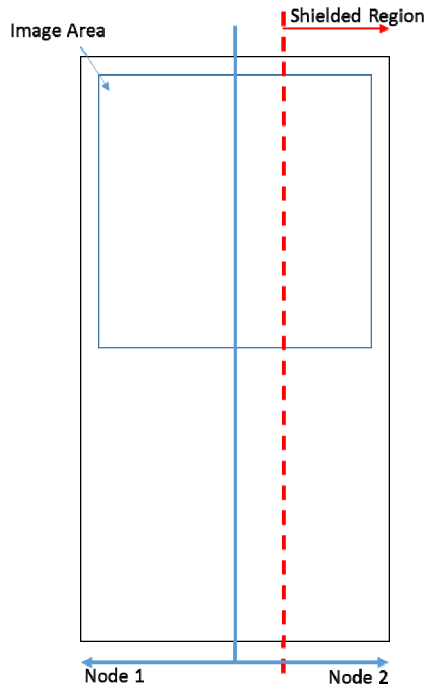
Figure 5. Schematic of the irradiated regions and output nodes of the 1 MeV electron irradiated CCD 47-20.
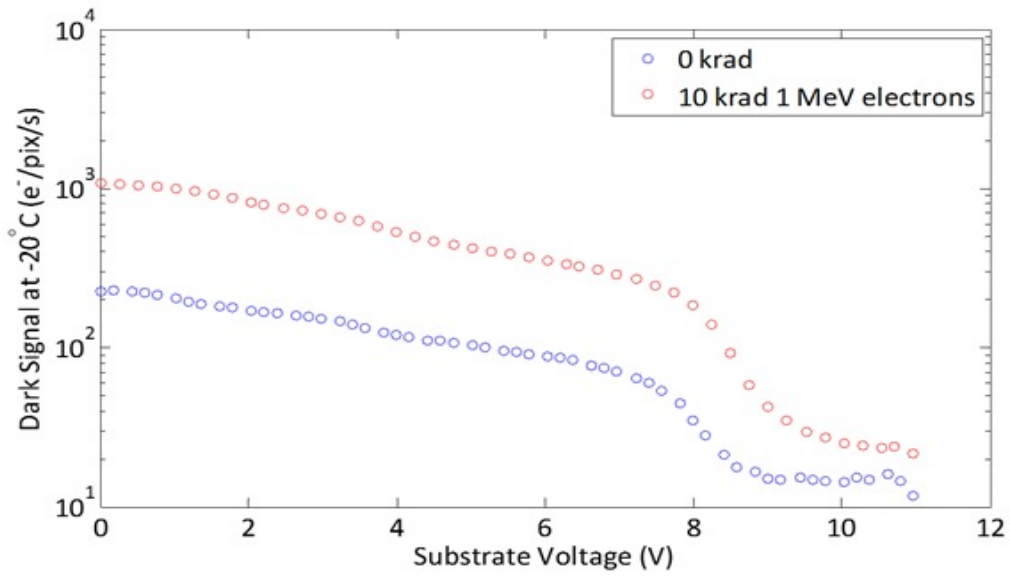


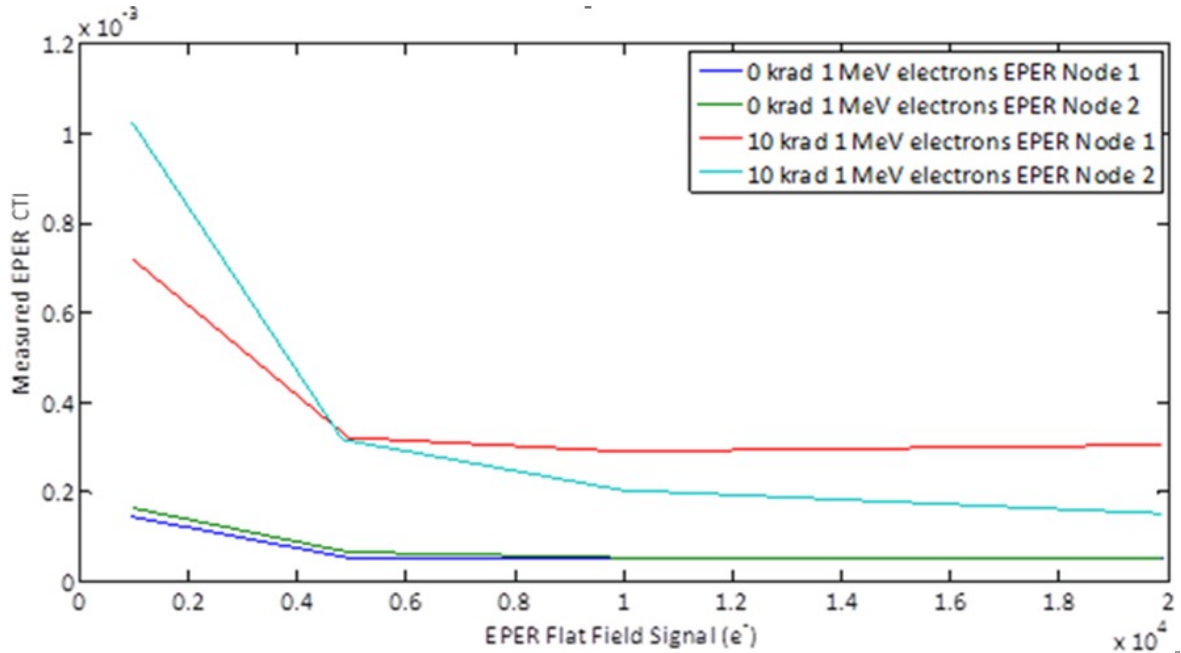Figure 6. Dark current as a function of substrate voltage at -20°C, before (blue) and after (red) irradiation to 10 krad of 1 MeV electrons.

Figure 7. EPER as a function of flat field signal at -20°C, before (blue, green) and after (red, cyan) irradiation to 10 krad of 1 MeV electrons
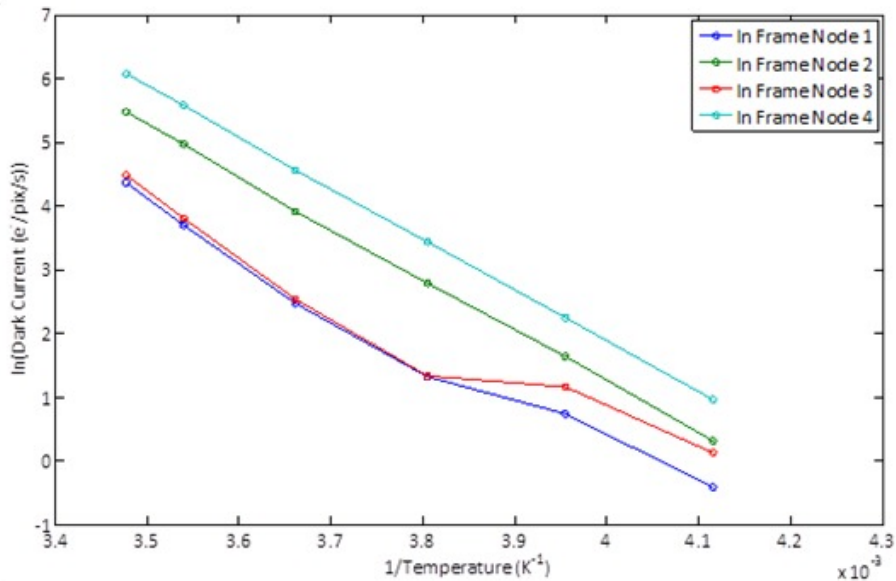


Figure 8. Dark current as a function of temperature, presented as an Arrhenius plot.

When considering proton irradiations, because of the higher effective NIEL, pixels exhibiting Random Telegraph Signal (RTS) become of concern. Figure 9 shows the signal over time (at approximately 0.5 frames/s) for selected pixels from a device irradiated with 72 MeV protons to 3 krad. In comparison, no RTS pixels were detected in an equivalent area on the electron irradiated device. The study will give important information for the susceptibility of the device to RTS creation under high energy electron irradiation.
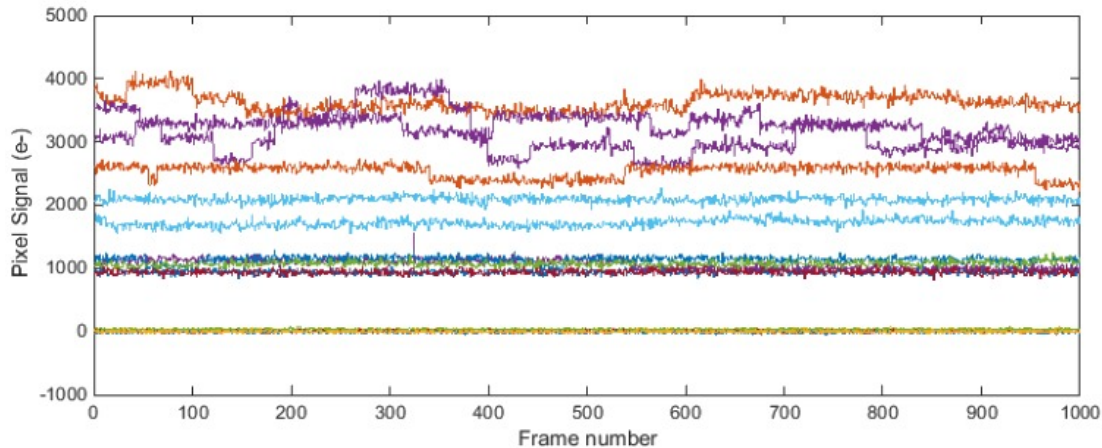
Figure 9. Example detected RTS pixels in a device irradiated to 3 krad with 72 MeV protons.

The results presented here show that the degradation of the CCD47-20 has been measured successfully, suggesting that the larger test campaign will be able to show the change in these metrics for a range of particle irradiations. Using these characteristics the NIEL factor will be compared between CCD, CIS, and PIPS photodiodes, and between 1, 6, 12, and 20 MeV electrons, with supporting evidence from proton (6.5, 72, and 200 MeV) and gamma (Cobalt 60) irradiations. This evidence will contribute to refining a high energy electron model of NIEL, which will contribute significantly to studies currently underway for future missions *e.g.* ESA's JUICE.

# 4. CONCLUSIONS

This paper shows preliminary results and progress towards a study to more accurately measure and model NIEL for high energy electrons. The preliminary results show radiation effects due to 1 MeV electrons in a CCD 47-20 and the effects are as expected following the initial analysis. The results will be able to be interpreted in more detail when the remaining irradiations are complete and all measurements are available for analysis, allowing a true comparison of high energy electron NIEL compared to the current model, for a range of devices.

The final results of the study will help to inform future irradiation campaigns and existing analysis of radiation damage measurements for mission going to hostile electron environments such as the Jovian system for the ESA JUICE mission.

# 5. ACKNOWLEDGEMENTS

# 6. REFERENCES

[1] A. Vasilescu and G. Lindstroem, *Displacement damage in silicon*, on-line compilation, http://rd50.web.cern.ch/RD50/NIEL/default.html, accessed 2016
[2] C. Inguimbert, P. Arnolda, T. Nuns, G. Rolland, *Effective NIEL in Silicon: Calculation using molecular dynamic results*, IEEE Trans. Nucl. Sci., vol. NS-57, no 4, pp. 1915-1923, 2010
[3] J. R. Srour, and D. H. Lo, *Universal damage factor for radiation-induced dark current in silicon devices,* IEEE Trans. Nucl. Sci., vol. NS-47, no 6, 2000.
[4] S. R. Messenger, E. M. Jackson, *et. al. Correlation of Telemetered Solar Array Data With Particle Detector Data On GPS Spacecraft,* IEEE Trans. Nucl. Sci., vol. NS-58,no 6, pp. 3118-3125, 2011
[5] C. Inguimbert, P. Arnolda, T. Nuns, G. Rolland, *Effective NIEL in Silicon: Calculation using molecular dynamic results*, IEEE Trans. Nucl. Sci., vol. NS-57, no 4, pp. 1915-1923, 2010.
[6] C. Inguimbert, S. Messenger, *Equivalent Displacement Damage Dose for On-Orbit Space Application,*Nuclear Science, IEEE Transactions on, Volume: 59, Issue: 6, Part: 1, pp. 3117 – 3125, 2012

[7]   V. Della Corte, N. Schmitz, M. Zusi, *et. al. The JANUS camera onboard JUICE mission for Jupiter system optical imaging,* Space Telescopes and Instrumentation 2014: Optical, Infrared, and Millimeter Wave, article no. 91433I

[8]   J. R. Srour, C. J. Marshall, P. W. Marshall, *Review of Displacement Damage Effects in Silicon Devices*, IEEE Transactions on Nuclear Science, Vol. 50, No. 3, June 2003

[9]   e2v technologies data sheet, *CCD47–20 Back Illuminated High Performance AIMO Back Illuminated CCD Sensor,* A1A-100041 Version 7, September 2007

[10] G. P. Summers, E. A. Burke, P. Shapiro, S. R. Messenger, R. J. Walters, *Damage correlations in semiconductors exposed to gamma, electron and proton radiations*, IEEE Trans. Nucl. Sci., vol. NS-40, no. 6, pp. 1372-1379, December 1993.